Phosphorylation of kinesin light chain 1 at serine 460 modulates binding and trafficking of calsyntenin-1

Alessio Vagnoni, Lilia Rodriguez, Catherine Manser, Kurt J. De Vos* and Christopher C. J. Miller*,‡

MRC Centre for Neurodegeneration Research, Institute of Psychiatry, King's College London, PO Box 37, De Crespigny Park, Denmark Hill, London SE5 8AF, UK

*These authors contributed equally to this work
‡Author for correspondence (chris.miller@kcl.ac.uk)

Accepted 22 November 2010
Journal of Cell Science 124, 1032-1042

doi:10.1242/jcs.075168

Summary

Kinesin light chain 1 (KLC1) binds to the intracellular cytoplasmic domain of the type-1 membrane-spanning protein calsyntenin-1 (also known as alcadein-α) to mediate transport of a subset of vesicles. Here, we identify serine 460 in KLC1 (KLC1ser460) as a phosphorylation site and show that mutation of KLC1ser460 influences the binding of KLC1 to calsyntenin-1. Mutation of KLC1ser460 to an alanine residue, to preclude phosphorylation, increased the binding of calsyntenin-1, whereas mutation to an aspartate residue, to mimic permanent phosphorylation, reduced the binding. Mutation of KLC1ser460 did not affect the interaction of KLC1 with four other known binding partners: huntingtin-associated protein 1 isoform A (HAP1A), collapsin response mediator protein-2 (CRMP2), c-Jun N-terminal kinase-interacting protein-1 (JIP1) and kinase-D-interacting substrate of 220 kDa (Kidins220). KLC1ser460 is a predicted mitogen-activated protein kinase (MAPK) target site, and we show that extracellular-signal-regulated kinase (ERK) phosphorylates this residue in vitro. We also demonstrate that inhibition of ERK promotes binding of calsyntenin-1 to KLC1. Finally, we show that expression of the KLC1ser460 mutant proteins influences calsyntenin-1 distribution and transport in cultured cells. Thus, phosphorylation of KLC1ser460 represents a mechanism for selectively regulating the binding and trafficking of calsyntenin-1.

Key words: Kinesin light chain 1, Calsyntenin-1, MAPK, ERK, Axonal transport, Alzheimer's disease

Introduction

Active transport of cargoes is mediated by molecular motors that hydrolyse ATP; the coupling of ATP hydrolysis to conformational changes allows the motors to produce mechanical force and movement. Members of the kinesin superfamily represent one class of motor protein. They transport cargo along microtubule 'rails'; for most kinesins, transport is towards the plus-end of microtubules (Hirokawa and Noda, 2008). Kinesin-1 was the first family member to be identified and functionally comprises a tetramer of two kinesin-1 heavy chains (KHCs) and two kinesin light chains (KLCs). KHC comprises a globular N-terminal head domain, which binds to microtubules and has ATPase activity, a central α-helical neck and stalk, which mediate KHC dimerisation, and a C-terminal tail region (Hirokawa and Noda, 2008). KLC1 is the best-studied KLC; it is ubiquitously expressed and contains a number of heptad repeats, located toward its N-terminus, and a series of tetratricopeptide repeat (TPR) domains in the C-terminal half of the molecule. KHC and KLC1 interact through domains in the KHC stalk and tail regions and the KLC1 N-terminal domain, including the heptad repeats; cargoes bind either directly to the C-terminus of KHC or do so through KLC1, especially its TPR domains (for a review, see Hirokawa and Noda, 2008).

Kinesin-1 transports a large number of cargoes, including components of the cytoskeleton, mitochondria and a diverse array of membrane-bound vesicles (Hirokawa and Noda, 2008). How a single motor can selectively attach, transport and release such different cargoes is not properly understood. One method involves differential exon splicing of *KLC1* mRNAs, as this produces isoforms that display cargo-specific binding (Wozniak and Allan, 2006). A further possibility is that post-translational modifications influence the attachment and release of cargoes; indeed KHC (Hollenbeck, 1993; Lee and Hollenbeck, 1995; Morfini et al., 2009; Sato-Yoshitake et al., 1992; Stagi et al., 2006), KLC1 (De Vos et al., 2000; Lindesmith et al., 1997; Matthies et al., 1993) and KLC2 (Ichimura et al., 2002; Morfini et al., 2002) are all phosphoproteins. Furthermore, there is evidence that phosphorylation of KLC2 influences binding of vesicular cargo (Ichimura et al., 2002; Morfini et al., 2002) and Ca^{2+}/calmodulin-dependent protein kinase II (CaMKII) has been shown to phosphorylate the kinesin-2 family member KIF17 in order to induce the release of cargo (Guillaud et al., 2007). However, to date there is no evidence that phosphorylation of KLC1 affects its binding to cargoes.

Calsyntenin-1 (also known as alcadein-α) is an evolutionarily conserved type-1 membrane-spanning protein that interacts with KLC1 through sequences in its C-terminal intracellular domain (Araki et al., 2007; Konecna et al., 2006). Calsyntenin-1 is widely expressed but is particularly abundant in the nervous system, where it is present in most neuronal subtypes (Hintsch et al., 2002). As a direct binding partner for KLC1, calsyntenin-1 has been implicated in the transport of a subset of vesicles and especially vesicles undergoing transport through axons of neurons (Araki et al., 2007; Konecna et al., 2006; Ludwig et al., 2009).

Here, we identify KLC1ser460 as a phosphorylated residue and show that mutation of this site to preclude or mimic phosphorylation selectively influences the binding of calsyntenin-1. We also show that KLC1ser460 is targeted by ERK and that mutation of KLC1ser460 alters the distribution and trafficking of calsyntenin-1. Phosphorylation of KLC1ser460 thus represents a mechanism for regulating transport of calsyntenin-1 cargoes.

Journal of Cell Science

Results

KLC1 is phosphorylated on serine 460

To identify phosphorylation sites within KLC1, we used mass spectrometry to sequence FLAG-tagged KLC1 (FLAG–KLC1) isolated from transfected Chinese hamster ovary (CHO) cells by immunoprecipitation using the FLAG tag. Following trypsin digestion, we obtained 91% sequence coverage and identified serine 460 as a phosphorylation site within the peptide ACKVDS*PTVTTTLK (Fig. 1B). This sequence, including serine 460, is conserved in rodent and human KLC1. During the course of our study, others also identified KLC1ser460 as a phosphorylation site through mass spectrometry sequencing of the phosphoproteome (Daub et al., 2008; Dephoure et al., 2008), including in mouse brain (see http://www.phosida.com/). KLC1 and calsyntenin-1 are both enriched in neurons (DeBoer et al., 2008; Hintsch et al., 2002), so we additionally analysed phosphorylation of KLC1ser460 in endogenous KLC1 isolated by immunoprecipitation from cultured rat cortical neurons. Again, we identified KLC1ser460 as a phosphorylated residue (Fig. 1C). Thus, KLC1ser460 is an in vivo phosphorylation site in neurons.

Mutation of KLC1ser460 modulates binding of calsyntenin-1

To investigate the role of KLC1ser460 phosphorylation, we generated KLC1ser460 mutants and monitored their ability to interact with KHC and with different cargoes in immunoprecipitation assays from transfected CHO cells. We mutated serine 460 to an alanine residue (KLC1ser460ala), to preclude phosphorylation, or to an aspartate residue (KLC1ser460asp), to mimic permanent phosphorylation [there are many examples whereby replacing serine residues with a negatively charged residue, such as an aspartate residue, accurately mimics the effect of phosphorylation of the site (e.g. Ackerley et al., 2003)].

We first monitored the effect of mutating KLC1ser460 on its binding to KHC; transfected FLAG–KLC1 was specifically immunoprecipitated using the FLAG tag. Wild-type KLC1 (KLC1wt), KLC1ser460ala and KLC1ser460asp all interacted equally well with endogenous KHC in these assays, and no signals for either KLC1 or KHC were obtained from control (empty-vector-transfected) cells, demonstrating the specificity of the immunoprecipitations (Fig. 2A). Serine 460 is located towards the C-terminus of KLC1, just N-terminal to the sixth TPR domain (Fig. 1A), and this region is not believed to directly mediate binding to KHC. Rather, the N-terminal domain of KLC1, including the heptad repeats, has been shown to bind KHC (Gauger and Goldstein, 1993; Verhey et al., 1998). The lack of effect of mutating KLC1ser460 on KHC binding is thus consistent with our current knowledge of the KLC1–KHC interaction.

We next studied whether mutation of KLC1ser460 influences binding to calsyntenin-1 given that the C-terminal portion of KLC1, which contains the six TPR domains and encompasses serine 460, is known to mediate this interaction (Araki et al., 2007; Konecna et al., 2006). For comparison, we also studied binding of the KLC1ser460 mutants with four other known partners that interact directly with KLC1. These were huntingtin-associated protein 1 isoform A (HAP1A), collapsin response mediator protein-2 (CRMP2; also know as DPYSL2), c-Jun N-terminal kinase-interacting protein-1 (JIP1) and kinase-D-interacting substrate of 220 kDa (Kidins220; also known as ARMS); the interaction of these cargoes is likewise believed to involve at least some of the TPR domains (Bowman et al., 2000; Bracale et al., 2007; Kimura et al., 2005; McGuire et al., 2005; Verhey et al., 2001). We co-transfected CHO cells with epitope-tagged cargo and FLAG-tagged KLC1wt, KLC1ser460ala or KLC1ser460asp, and monitored binding of cargo following immunoprecipitation of KLC1 through the FLAG tag. Cargoes were detected through their epitope tags. Control experiments in which either KLC1 or cargo were omitted

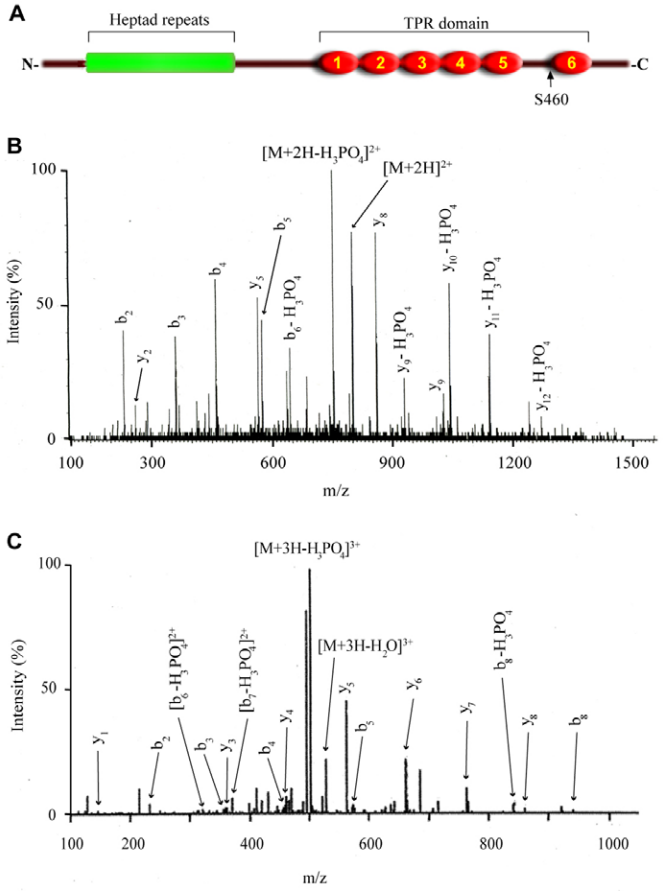

Fig. 1. Identification of KLC1ser460 as a phosphorylation site by LC–MS/MS. (**A**) A schematic representation of the KLC1 structure showing the heptad repeats (green box) and the TPR domain (comprising six tandem repeats numbered 1–6). Serine 460 (S460) is located in a linker region between TPR domains 5 and 6. (**B**,**C**) Tandem MS/MS spectra of the KLC1 phosphopeptide ACKVDSPTVTTTLK fragment ion series, after collision-induced dissociation. (B shows the spectrum with transfected FLAG–KLC1 and C shows that with endogenous KLC1 isolated from rat cortical neurons). The *m*/*z* of the fragment ions is plotted against the intensity, and the detected ions of the b- and y-ion collision series are indicated. The pattern of fragment ions produced localises the phosphorylation site in both samples to serine 460. (B) The mass difference between y_8 and y_9 and the release of phosphoric acid from y_9 (y_9-H_3PO_4) is consistent with a phosphorylation on serine 460. $[M+2H]^{2+}$ represents the peptide ion with *m*/*z*=800.9, used as the parent ion for fragmentation to produce the MS/MS spectrum; $[M+2H-H_3PO_4]^{2+}$ indicates the neutral loss of phosphoric acid. (C) Neutral loss from b_6 ($[b_6-H_3PO_4]^{2+}$) but not from y_1 to y_8 localises the phosphorylation site to serine 460. Consecutively matched y-ions without neutral loss indicate no phosphorylation of other potential sites (threonine 462, threonine 464, threonine 465 and threonine 466). The parent ion is absent following the fragmentation. $[M+3H-H_2O]^{3+}$ at *m*/*z*=528.12 and $[M+3H-H_3PO_4]^{3+}$ at *m*/*z*=501.39 represent the loss of water and the neutral loss of phosphoric acid from the parent ion, respectively.

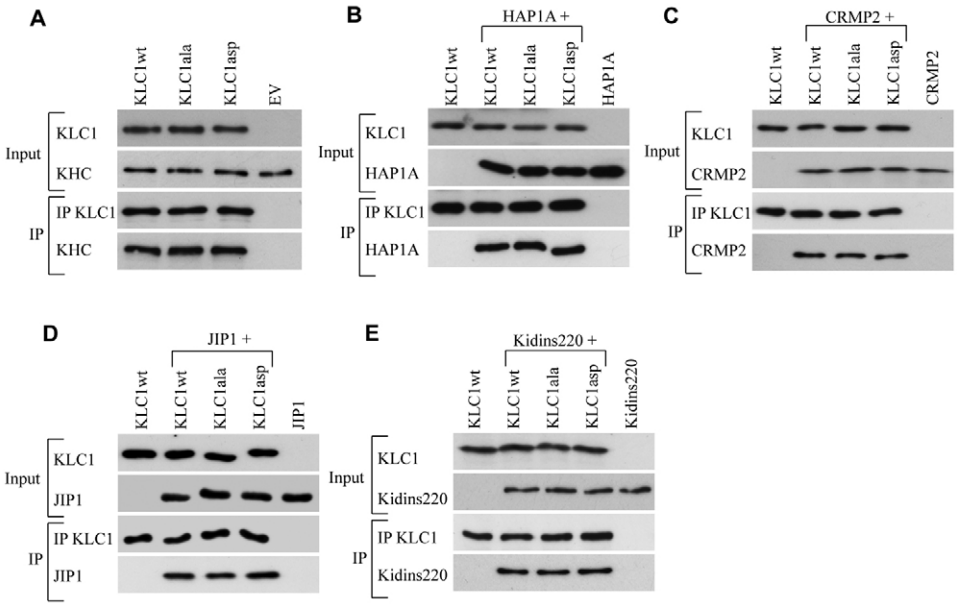

Fig. 2. Mutation of KLC1ser460 into alanine or aspartate residues does not affect the binding of KLC1 to KHC or to HAP1A, CRMP2, JIP1 or Kidins220. (**A**) CHO cells were transfected with FLAG–KLC1wt, FLAG–KLC1ser460ala (KLC1ala), FLAG–KLC1ser460asp (KLC1asp) or empty vector (EV), and KLC1 was immunoprecipitated (IP) using the anti-FLAG antibody. Samples were probed on immunoblots for KLC1, using anti-FLAG antibody, and for endogenous KHC, using the antibody pcp42. (**B**–**E**) CHO cells were co-transfected with FLAG–KLC1wt, FLAG–KLC1ser460ala or FLAG–KLC1ser460asp and Myc–HAP1A (B), Myc–CRMP2 (C), Myc–JIP1 (D) or EGFP–Kidins220 (E). KLC1 was immunoprecipitated using the anti-FLAG antibody. The samples were probed on immunoblots for KLC1, using anti-FLAG antibody, and bound cargoes, using anti-Myc or anti-GFP antibodies. To demonstrate the specificity of the immunoprecipitations, cells were also singly transfected with KLC1wt, or with Myc–HAP1A (B), Myc–CRMP2 (C), Myc–JIP1 (D) or EGFP–Kidins220 (E). Samples of the input lysates and immunoprecipitates are shown.

from the transfections demonstrated the specificity of the immunoprecipitations. Mutation of serine 460 did not alter binding of KLC1 to HAP1A, CRMP2, JIP1 or Kidins220 (Fig. 2B–E). However, mutation of serine 460 consistently altered binding of KLC1 to calsyntenin-1 (Fig. 3A). Quantification of signals from the immunoblots revealed that KLC1ser460ala bound approximately twofold more and KLC1ser460asp bound approximately twofold less calsyntenin-1 than KLC1wt in these assays (KLC1ser460ala versus KLC1wt, 2.05±0.27-fold increase, $P<0.001$; KLC1ser460asp versus KLC1wt, 1.98±0.25-fold decrease $P=0.027$. One-way ANOVA, $n=4$. Fold changes are ±s.d.) (Fig. 3A). To confirm further the selective effect of mutating KLC1ser460 on binding of calsyntenin-1, we performed the reverse experiment and immunoprecipitated calsyntenin-1 using the EGFP-tag and probed for FLAG–KLC1. Again, quantification of signals from immunoblots revealed that calsyntenin-1 bound approximately twofold more KLC1ser460ala and twofold less KLC1ser460asp than KLC1wt (KLC1ser460ala versus KLC1wt, 2.17±0.13-fold increase, $P<0.001$; KLC1ser460asp versus KLC1wt, 1.96±0.27-fold decrease, $P=0.021$. One-way ANOVA, $n=4$. Fold changes are ±s.d.) (Fig. 3A).

The functional kinesin-1 tetramer is now known to comprise two homodimers, each containing a single KLC isoform (KLC1 or KLC2); heterotetramers containing both KLC1 and KLC2 do not exist in vivo (DeBoer et al., 2008). Transfection of KLC1wt, KLC1ser460ala or KLC1ser460asp greatly increased KLC1 expression (Fig. 3B) and, as such, most of the functional kinesin-1 tetramers in the transfected cells probably comprise KHC and transfected KLC1. However, a proportion of these tetramers might be mixed (i.e. containing one molecule of transfected KLC1 and one molecule of endogenous wild-type KLC1). To eliminate the possibility that this mixture influences the amounts of calsyntenin-1 bound to the KLC1 phosphorylation mutants in the immunoprecipitation experiments, we analysed the amounts of calsyntenin-1 bound to transfected KLC1wt, KLC1ser460ala or KLC1ser460asp in cells where expression of endogenous KLC1 was reduced using small interfering RNA (siRNA). For these experiments we utilised human embryonic kidney HEK-293 cells and an siRNA that specifically targets human KLC1 but not the transfected mouse KLC1 (owing to four mismatches between the mouse and human sequences in the siRNA). siRNA treatment decreased expression of endogenous KLC1 by over 90% but, as predicted, had no effect on transfected mouse KLC1 (Fig. 3C). Cells were then treated with human-specific KLC1 siRNA and co-transfected with EGFP–calsyntenin-1 and FLAG-tagged KLC1wt, KLC1ser460ala or KLC1ser460asp. KLC1 was immunoprecipitated from the cells and the amounts of bound calsyntenin-1 detected by immunoblotting. As in the previous experiments, scanning of immunoblots revealed that KLC1ser460ala bound approximately twofold more and KLC1ser460asp approximately twofold less calsyntenin-1 than KLC1wt in these assays (Fig. 3D). Thus, mutation of KLC1ser460, in order to preclude or mimic permanent phosphorylation, regulates KLC1 binding to calsyntenin-1. Moreover, this effect is selective for calsyntenin-1 and not four other known cargo proteins.

KLC1ser460 is phosphorylated by ERK and inhibition of ERK increases binding of KLC1 to calsyntenin-1

KLC1ser460 falls within a consensus sequence for phosphorylation by ERK (see, e.g. http://www.phosida.com/). We therefore investigated whether inhibition of ERK activity influenced the amount of calsyntenin-1 that binds to immunoprecipitated FLAG–

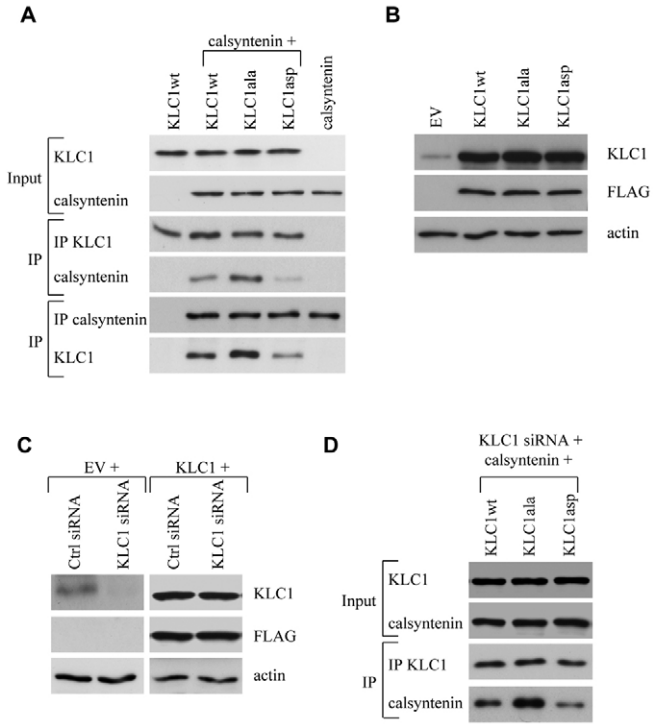

Fig. 3. Mutation of KLC1ser460 to alanine or aspartate residues alters the binding of KLC1 to calsyntenin-1. (**A**) Cells were co-transfected with EGFP–calsyntenin-1 (calsyntenin) and either FLAG–KLC1wt, FLAG–KLC1ser460ala (KLC1ala) or FLAG–KLC1ser460asp (KLC1asp). KLC1 was immunoprecipitated (IP) using the anti-FLAG antibody and calsyntenin-1 was immunoprecipitated using the anti-GFP antibody. The samples were then probed on immunoblots for KLC1, using the anti-FLAG antibody, and for calsyntenin-1, using the anti-GFP antibody. To demonstrate the specificity of the immunoprecipitations, cells were also singly transfected with either FLAG–KLC1wt or EGFP–calsyntenin-1. Samples of the input lysates and immunoprecipitates are shown. In both immunoprecipitation assays, KLC1ser460ala bound approximately twofold more and KLC1ser460asp bound approximately twofold less calsyntenin-1 than KLC1wt. (**B**) Transfection of FLAG–KLC1 markedly increases KLC1 expression. Cells were transfected with empty vector (EV) or FLAG-tagged KLC1wt, KLC1ala or KLC1asp; total and transfected KLC1 was detected on immunoblots using anti-KLC1 and anti-FLAG antibodies as indicated. The samples were also probed for actin as a loading control. (**C**) siRNA-mediated knockdown of endogenous human but not transfected mouse FLAG–KLC1 in HEK-293 cells. Cells were co-transfected with either empty vector (EV) or FLAG–KLC1, and either control siRNA (Ctrl) or human-specific KLC1 siRNA as shown. Samples were probed on immunoblots for total KLC1 (KLC1) and transfected FLAG–KLC1 using the anti-FLAG antibody as indicated. The samples were also probed for actin as a loading control. (**D**) KLC1ser460ala binds approximately twice, and KLC1ser460asp binds approximately half, the calsyntenin-1 than KLC1wt following siRNA-mediated knockdown of endogenous KLC1. Cells were co-transfected with EGFP–calsyntenin-1 (calsyntenin) and human-specific KLC1 siRNA, and mouse FLAG–KLC1wt (KLC1wt), FLAG–KLC1ser460ala (KLC1ala) or FLAG–KLC1ser460asp (KLC1asp). KLC1 was immunoprecipitated using anti-FLAG antibody and the input and immunoprecipitate samples probed on immunoblots for KLC1, using the anti-FLAG antibody, and calsyntenin-1, using anti-GFP antibody.

KLC1 in co-transfected cells; inhibiting the kinase responsible for phosphorylating KLC1ser460 would be predicted to alter the binding of KLC1 to calsyntenin-1 in a manner similar to that of the KLC1ser460ala mutant. Treatment of cells with U0126, a specific inhibitor of ERK, increased the amount of calsyntenin-1 that bound to FLAG–KLC1wt. However, U0126 had no effect on the binding of calsyntenin-1 to FLAG–KLC1ser460ala, which mimics a permanently non-phosphorylated state on residue 460 and therefore would not be expected to be affected by inhibition of ERK (Fig. 4A). Taken together, these observations support the notion that ERK regulates binding of KLC1 to calsyntenin-1 and that this involves phosphorylation of KLC1ser460.

To determine whether, under normal physiological conditions, inhibition of other members of the MAPK family also influences the binding of KLC1 to calsyntenin-1, we performed similar immunoprecipitations from co-transfected cells in which the activities of the stress-activated kinases p38 and c-Jun N-terminal kinase (JNK) were inhibited. p38 was inhibited with SB203580 and JNK with SP600125. Inhibition of p38 or JNK had no effect on binding of FLAG–KLC1 to EGFP–calsyntenin-1 (Fig. 4B,C).

The above studies strongly suggest that ERK phosphorylates KLC1ser460. To obtain more-direct evidence in support of this possibility, we performed in vitro phosphorylation assays with recombinant KLC1 substrates and ERK. KLC1(154–534) (which spans the TPR domains and includes KLC1ser460) and mutant KLC1(154–534)ser460ala, which cannot be phosphorylated on serine 460, were prepared and phosphorylated in vitro with [γ-^{32}P]ATP and ERK. ERK phosphorylated KLC1(154–534) but not KLC1(154–534)ser460ala (Fig. 4D). Thus, ERK phosphorylates KLC1ser460.

Finally, we tested whether inhibition of ERK promoted binding of endogenous kinesin-1 to endogenous calsyntenin-1. To do so, primary rat cortical neurons were treated with either vehicle or U0126, and the amount of calsyntenin-1 bound to immunoprecipitated kinesin-1 motors was determined. We chose neurons for this study, as they express a high level of calsyntenin-1 (Hintsch et al., 2002). KHC was immunoprecipitated using antibody SUK4 and the amounts of bound KLC1 and calsyntenin-1 monitored. Treatment with U0126 had no effect on binding of KHC to KLC1, which demonstrates that inhibition of ERK does not induce a global change in the KHC–KLC1 complex. However, U0126 increased the amount of calsyntenin-1 bound to the kinesin-1 motor by 2.33-fold (P=0.004, n=3, as determined by a Student's t-test) (Fig. 4E). ERK therefore regulates the amount of calsyntenin-1 cargo attached to the kinesin-1 motor complex but has no overall effect on the binding of KLC1 to KHC.

Mutation of KLC1ser460 alters the colocalisation of KLC1 with calsyntenin-1

Calsyntenin-1 has been shown to recruit kinesin-1 to the Golgi and mediate post-Golgi transport of calsyntenin-1-containing vesicles to the cell surface (Araki et al., 2007; Konecna et al., 2006; Ludwig et al., 2009). The above biochemical studies, which show that phosphorylation of KLC1ser460 alters the binding of calsyntenin-1 to KLC1, suggest that this phosphorylation regulates kinesin-1-mediated trafficking of calsyntenin-1. To explore this possibility, we studied the intracellular distribution of EGFP–calsyntenin-1 together with FLAG-tagged KLC1wt, KLC1ser460ala or KLC1ser460asp in transfected CV-1 cells (CV-1 cells are particularly suitable for such studies owing to their highly spread morphology).

We first monitored the distribution of transfected calsyntenin-1. Calsyntenin-1 localised to vesicular structures distributed throughout the cytoplasm but was particularly prominent in perinuclear regions. Co-staining for the endoplasmic reticulum

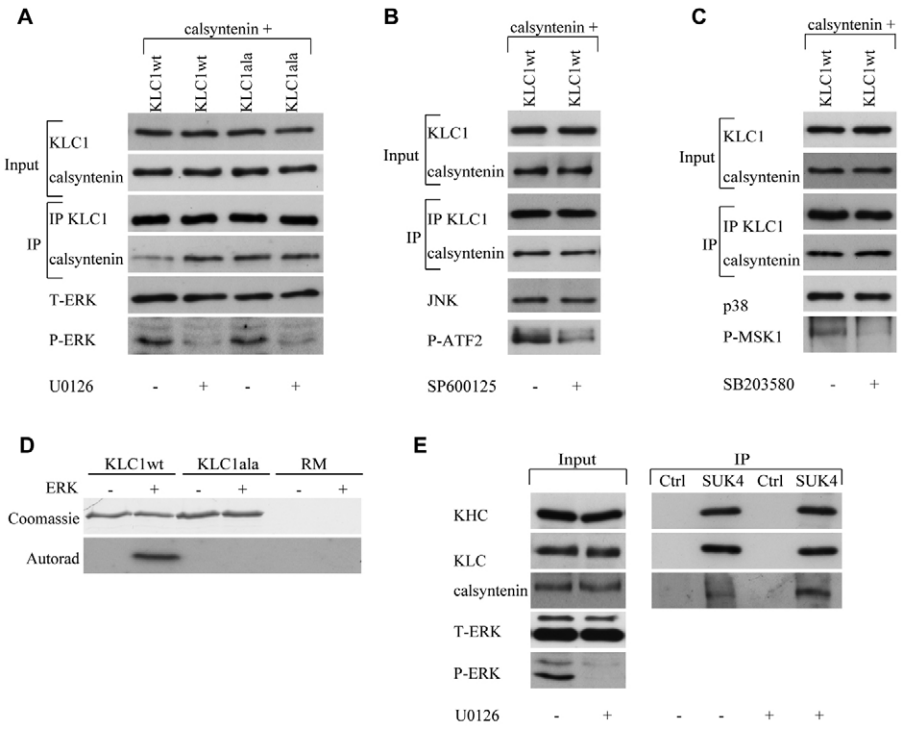

Fig. 4. KLC1ser460 is phosphorylated by ERK and inhibition of ERK increases binding of KLC1 to calsyntenin-1. (**A**) Inhibition of ERK promotes binding of calsyntenin-1 to KLC1wt but has no effect on its binding to KLC1ser460ala in immunoprecipitation (IP) assays from co-transfected CHO cells. Cells were co-transfected with EGFP–calsyntenin-1 (calsyntenin) and either FLAG–KLC1wt (KLC1wt) or FLAG-KLC1ser460ala (KLC1ala), and the cells were then treated (+) or not treated (–) with U0126 to inhibit ERK. KLC1 was immunoprecipitated using the anti-FLAG antibody and the samples were probed on immunoblots for KLC1, using the anti-FLAG antibody, and calsyntenin-1, using the anti-GFP antibody. Samples of the input lysates and immunoprecipitates are shown. Also shown are immunoblots for total and active ERK (T-ERK and P-ERK, respectively). (**B**,**C**) Inhibition of JNK (B) or p38 (C) does not influence binding of KLC1 to calsyntenin-1 in immunoprecipitation assays from co-transfected CHO cells. Cells were co-transfected with EGFP–calsyntenin-1 and FLAG–KLC1wt, and the cells were then treated (+) or not treated (–) with SP600125, to inhibit JNK (B), or SB203580, to inhibit p38 (C). KLC1 was immunoprecipitated using the anti-FLAG antibody, and the samples were probed on immunoblots for KLC1, using the anti-FLAG antibody, and calsyntenin-1, using the anti-GFP antibody. Samples of the input lysates and immunoprecipitates are shown. Also shown are immunoblots for total JNK (p54 isoform) and phosphorylated ATF2 (P-ATF2) in (B), to show JNK inhibition, and total p38 and phosphorylated MSK1 (P-MSK1) in (C), to show MAPK inhibition. ATF2 and MSK1 are downstream substrates for JNK and p38, respectively. (**D**) In vitro phosphorylation of KLC1(154–534) but not KLC1(154–534)ser460ala by ERK. KLC1wt or KLC1ser460ala substrates were prepared and phosphorylated in vitro with [γ-^{32}P]ATP and ERK. RM is reaction mix only with no substrate; – and + refer to the presence or absence of ERK in the reaction. The upper panel is a Coomassie-Blue-stained gel to show KLC1 substrates; the lower panel is the autoradiograph. (**E**) Inhibition of ERK promotes binding of endogenous calsyntenin-1 to endogenous kinesin-1 motors in immunoprecipitation assays from 7DIV rat cortical neurons. Kinesin-1 was immunoprecipitated using the SUK4 antibody, and bound KLC1 and calsyntenin-1 were detected on immunoblots using rabbit anti-KLC antibody and anti-calsyntenin-1 antibody, respectively; KHC was detected using H2. Control immunoprecipitations (Ctrl) were performed using non-immune mouse Igs. Samples of the input lysates and immunoprecipitates are shown. Also shown are immunoblots for total and active ERK; – and + represent absence or presence of U0126 treatment.

(ER) protein disulphide isomerase (PDI), cis-Golgi matrix protein-130 (GM130) and trans-Golgi network protein-46 (TGN-46) revealed that calsyntenin-1 was particularly enriched within the Golgi (Fig. 5A). These results are in agreement with previous studies (Ludwig et al., 2009).

Transfected FLAG–KLC1wt, FLAG–KLC1ser460ala and FLAG-KLC1ser460asp all gave a diffuse cytoplasmic labelling, with no noticeable differences in these labelling patterns between wild-type and mutant proteins (Fig. 5B). Others have reported similar cytoplasmic labelling for KLC1wt (Araki et al., 2007; Verhey et al., 1998).

In agreement with previous studies, cells co-transfected with very high levels of calsyntenin-1 and KLC1wt (as judged by the brightness of the fluorescence signal) formed large cytoplasmic structures of aberrant appearance that were labelled for both proteins and PDI (supplementary material Fig. S1); these have been described by others and are known to comprise abnormal ER stacks (Ludwig et al., 2009). However, in cells that express lower levels of calsyntenin-1 and KLC1wt the morphology was normal, with both proteins colocalising in perinuclear regions and in vesicular structures scattered throughout the cytoplasm (Fig. 6A). These results are again in accordance with previous studies, showing that the dual overexpression of calsyntenin-1 and KLC1wt induces their colocalisation (Araki et al., 2007; Ludwig et al., 2009). We therefore restricted our analyses to cells that expressed low levels of transfected calsyntenin-1 and KLC1 (as judged by the brightness of the fluorescence signal), which presented a normal phenotype.

KLC1 has been shown to mediate kinesin-1 transport of calsyntenin-1 to the cell periphery (Araki et al., 2007; Konecna et al., 2006; Ludwig et al., 2009). To confirm this finding, we first studied the distribution or EGFP–calsyntenin-1 in cells treated with either control siRNA or siRNA targeting KLC1. In cells treated with control siRNA, EGFP–calsyntenin-1 localised to

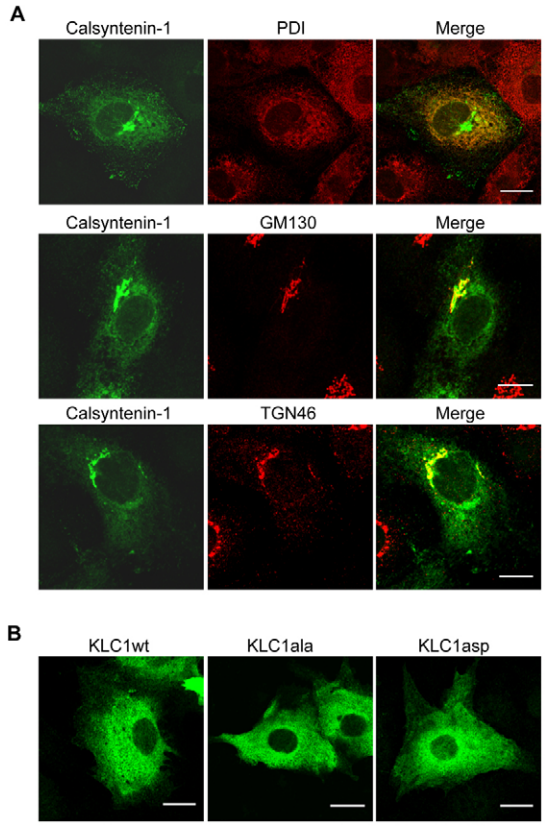

Fig. 5. Localisation of calsyntenin-1, and KLC1wt, KLC1ser460ala and KLC1ser460asp in transfected CV-1 cells. (**A**) Confocal images of cells transfected with EGFP–calsyntenin-1 and co-stained for PDI, GM130 or TGN-46. (**B**) Confocal images of CV1 cells transfected with FLAG–KLC1wt, FLAG–KLC1ser460ala (KLC1ala) or FLAG–KLC1ser460asp (KLC1asp). Scale bars: 20 µm.

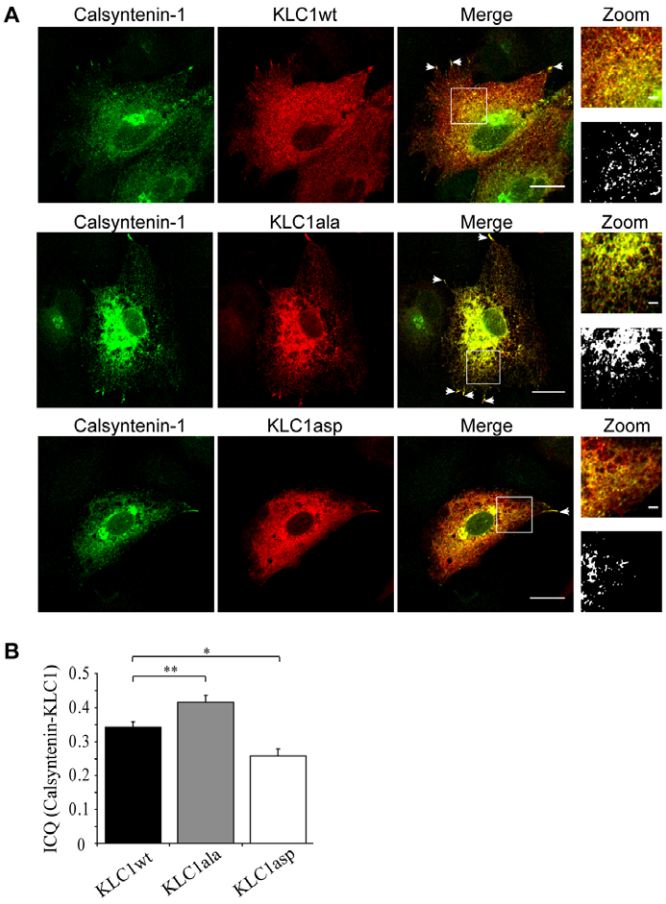

Fig. 6. Mutation of KLC1ser460 alters KLC1 co-localisation with calsyntenin-1 in transfected CV-1 cells. CV-1 cells were co-transfected with EGFP–calsyntenin-1 and FLAG–KLC1wt, FLAG–KLC1ser460ala (KLC1ala) or FLAG–KLC1ser460asp (KLC1asp). Calsyntenin-1 was detected through the EGFP tag and KLC1 using the anti-FLAG antibody; images shown are confocal sections. (**A**) Calsyntenin-1 is highly co-localised with wild-type and both mutant KLC1s in perinuclear regions. In addition calsyntenin-1 and FLAG–KLC1ser460ala co-localise in plasma membrane projections; such co-staining of projections was less commonly seen in calsyntenin-1 plus FLAG–KLC1ser460asp co-transfected cells (arrowheads). Magnified areas of interest are shown, with co-localised pixels shown in the lower zoom panel. (**B**) ICQ values for colocalisation of calsyntenin-1 with KLC1wt, KLC1ser460ala or KLC1ser460asp. Calsyntenin-1 with KLC1wt, ICQ 0.33±0.04 (n=10); calsyntenin-1 with KLC1ser460ala, ICQ 0.394±0.05 (n=10); calsyntenin-1 with KLC1ser460asp: ICQ 0.225±0.05 (n=10). Data were analysed by one-way ANOVA with a LSD post-hoc test (*P<0.05; **P<0.01). Values are means ± s.d. Scale bars: 20 µm (2.5 µm in zoom panels).

vesicular structures distributed throughout the cytoplasm, but was particularly prominent in perinuclear regions (as described above in cells transfected with EGFP–calsyntenin-1; see Fig. 5) (supplementary material Fig. S2A). However, treatment with KLC1 siRNA altered this distribution, such that EGFP–calsyntenin-1 was less readily apparent towards peripheral regions of the cytoplasm and instead appeared restricted to perinuclear regions (supplementary material Fig. S2B). These findings are thus consistent with a role for KLC1 in transporting calsyntenin-1 to the cell periphery and are in agreement with previous studies (Araki et al., 2007; Konecna et al., 2006; Ludwig et al., 2009).

We next quantified the degree of colocalisation of calsyntenin-1 with KLC1wt, KLC1ser460ala or KLC1ser460asp by using intensity correlation analyses (ICAs) as described previously (Li et al., 2004; Tudor et al., 2010). ICA yields an intensity correlation quotient (ICQ), which is a statistically testable single-value assessment of the relationship between two stained protein pairs: for dependent staining (colocalisation) 0<ICQ≤+0.5, for random staining ICQ=0 and for segregated staining 0>ICQ≥–0.5 (no colocalisation) (Li et al., 2004). To test whether ICQ values were significantly different from 0 we used a one-sample Student's t-test with the theoretical mean equal to 0; the obtained P values are indicated as P_{ICQ}. Cells co-transfected with calsyntenin-1 and KLC1wt, KLC1ser460ala or KLC1ser460asp all produced positive ICQ values, demonstrating partial but significant colocalisation between calsyntenin-1 and all of the KLC variants (P_{ICQ}<0.0001). However, the values for KLC1ser460ala and KLC1ser460asp colocalising with calsyntenin-1 were significantly higher and lower, respectively, than that for KLC1wt (Fig. 6B). These results thus complement the biochemical analyses and are consistent with KLC1ser460ala binding more, and KLC1ser460asp less, calsyntenin-1 than KLC1wt.

For comparison, we also monitored the distribution of HAP1A with KLC1wt, KLC1ser460ala and KLC1ser460asp in co-transfected CV-1 cells (supplementary material Fig. S3). We chose HAP1A as an example of a cargo whose binding to KLC1 was

unaffected by serine 460 phosphorylation in the biochemical assays. HAP1A has been shown to colocalise with kinesin-1 in co-transfected cells (McGuire et al., 2005). As with calsyntenin-1, cells co-transfected with HAP1A and KLC1wt, KLC1ser460ala or KLC1ser460asp all produced positive ICQ values demonstrating partial but significant colocalisation (P_{ICQ}<0.0001). However, unlike calsyntenin-1 there were no detectable differences between these values, and we detected no noticeable differences in staining patterns between the different transfections (supplementary material Fig. S3A,B). Again, these results complement the biochemical analyses.

In the course of the above studies, we noticed that cells co-transfected with calsyntenin-1 and either KLC1wt or KLC1ser460ala not only showed colocalised staining in perinuclear regions and cytoplasmic structures but also showed colocalised staining in areas towards the cell periphery. In particular, cells transfected with calsyntenin-1 and KLC1ser460ala commonly showed co-staining for both proteins at the tips of plasma membrane projections (Fig. 6A). By contrast, cells co-transfected with calsyntenin-1 and KLC1ser460asp showed colocalised staining in perinuclear areas but calsyntenin-1 labelling was less frequently observed at the cell periphery in such projections (Fig. 6A). Others have also shown that transfected KLC1wt and calsyntenin-1 colocalise in plasma membrane projections and have concluded that this is indicative of kinesin-1-mediated transport of calsyntenin-1 to the cell surface (Araki et al., 2007). We therefore quantified this phenotype by counting the numbers of calsyntenin-1 and KLC1 co-stained projections in co-transfected cells. Compared with cells co-transfected with calsyntenin-1 and KLC1wt, those transfected with calsyntenin-1 and KLC1ser460ala cells had significantly more co-stained projections, whereas cells transfected with calsyntenin-1 plus KLC1ser460asp had significantly less co-stained projections [calsyntenin-1 plus KLC1wt, 2.46(±1.1) co-stained projections per cell; calsyntenin-1 plus KLC1ser460ala, 3.96(±1.86) co-stained projections per cell; calsyntenin-1 plus KLC1ser460asp 1.63(±0.8) co-stained projections per cell; P<0.05, KLC1wt compared with KLC1ser460ala; P<0.001, KLC1wt compared with KLC1ser460asp (as determined using one-way ANOVA and n=90 cells in three different transfection experiments)].

Mutation of KLC1ser460 modulates calsyntenin-1 transport through axons of transfected neurons

Taken together, the above observations suggest that the mutation of KLC1ser460 alters the transport of calsyntenin-1. To examine this in more detail, we monitored axonal transport of EGFP–calsyntenin-1 in rat cortical neurons co-transfected with KLC1wt, KLC1ser460ala or KLC1ser460asp through time-lapse microscopy. Calsyntenin-1 is enriched in neurons and is transported in an anterograde manner through axons by kinesin-1 (Araki et al., 2007; Konecna et al., 2006). Again, we selected cells that expressed low-levels of calsyntenin-1 (as judged by the EGFP signal) for analyses so as to avoid any possible artefacts produced by high levels of expression of calsyntenin-1. To confirm that the cells transfected with EGFP–calsyntenin-1 were also co-transfected with low levels of KLC1, we immunostained the coverslips for the FLAG tag on the KLC1 following the imaging. These experiments revealed that over 95% of EGFP–calsyntenin-1-positive neurons were co-transfected with KLC1, which is in accordance with many other studies (e.g. De Vos et al., 2007).

EGFP–calsyntenin-1 moved bidirectionally through axons and the mean speed of movement was not significantly different between cells co-transfected with KLC1wt, KLC1ser460ala or KLC1ser460asp (EGFP–calsyntenin plus KLC1wt, 1.24±0.27 μm/second anterograde, 0.73±0.24 μm/second retrograde; EGFP–calsyntenin-1 plus KLC1ser460ala, 1.32±0.35 μm/second anterograde, 0.83±0.36 μm/second retrograde; EGFP–calsyntenin-1 plus KLC1ser460asp, 1.15±0.36 μm/second anterograde, 0.81±0.37 μm/second retrograde; values are means ± s.d.]. These velocities are similar to those described by others (Araki et al., 2007; Konecna et al., 2006). We also found that ~77% of moving EGFP–calsyntenin-1 particles (in cells co-transfected with KLC1wt) were transported in an anterograde direction, which is a similar proportion to that reported previously (Araki et al., 2007; Konecna et al., 2006). However, when we calculated the proportions of moving EGFP–calsyntenin-1 carriers travelling in anterograde and retrograde directions, we found that co-transfection of KLC1ser460ala increased, whereas KLC1ser460asp decreased, the relative proportions of anterogradely moving EGFP–calsyntenin-1 compared with that in cells co-transfected with KLC1wt (Fig. 7A,B). Conversely, the relative proportions of retrogradely moving EGFP–calsyntenin-1 were increased in the presence of KLC1ser460asp and decreased in the presence of KLC1ser460ala compared with that in cells co-transfected with KLC1wt (Fig. 7A,C). Thus, mutation of KLC1ser460 to preclude or mimic permanent phosphorylation modulates colocalisation of KLC1 with calsyntenin-1 and axonal transport of calsyntenin-1.

Discussion

The mechanisms by which kinesins selectively transport different cargoes to their appropriate subcellular sites of action, and how this transport is regulated in response to physiological stimuli, are not properly understood. For kinesin-1, one tier of control involves modulating the binding of KHC to microtubule rails; tubulin acetylation has been shown to promote binding of KHC to enhance transport (Dompierre et al., 2007; Reed et al., 2006), whereas phosphorylation of KHC on serine176 by JNK3 reduces its binding to microtubules and inhibits transport (Morfini et al., 2009). Perturbation of both these processes has been shown to contribute to defective axonal transport in Huntington's disease (Dompierre et al., 2007; Morfini et al., 2009). In addition, binding of cargo to KLCs can also influence KHC–microtubule interactions. In one model, in the absence of cargo, KLC and KHC interact to inhibit binding of the motor complex to microtubules, and thus stop kinesin movement, but loading of cargo induces a conformational change that permits binding to microtubules and activates the motor function (Stock et al., 1999; Verhey et al., 1998).

A second tier of control involves the regulation of cargo binding to KLCs. C-terminal splice variants of KLC1 display cargo-specific interactions (Wozniak and Allan, 2006), and phosphorylation of KLC2 has been shown to both inhibit and promote cargo binding. Thus, phosphorylation of KLC2 by glycogen synthase kinase-3β inhibits binding and transport of some vesicular cargoes (Morfini et al., 2002), whereas phosphorylation of KLC2 on serine575 stimulates binding of 14-3-3 protein cargo (Ichimura et al., 2002).

Here, we show for the first time that phosphorylation of KLC1 can also regulate the binding and transport of cargo. We identify KLC1ser460 as an in vivo phosphorylation site and demonstrate that mutation of this site regulates the binding of calsyntenin-1. Mutation of KLC1ser460 to an alanine residue, to preclude phosphorylation, increased the binding of KLC1 to calsyntenin-1,

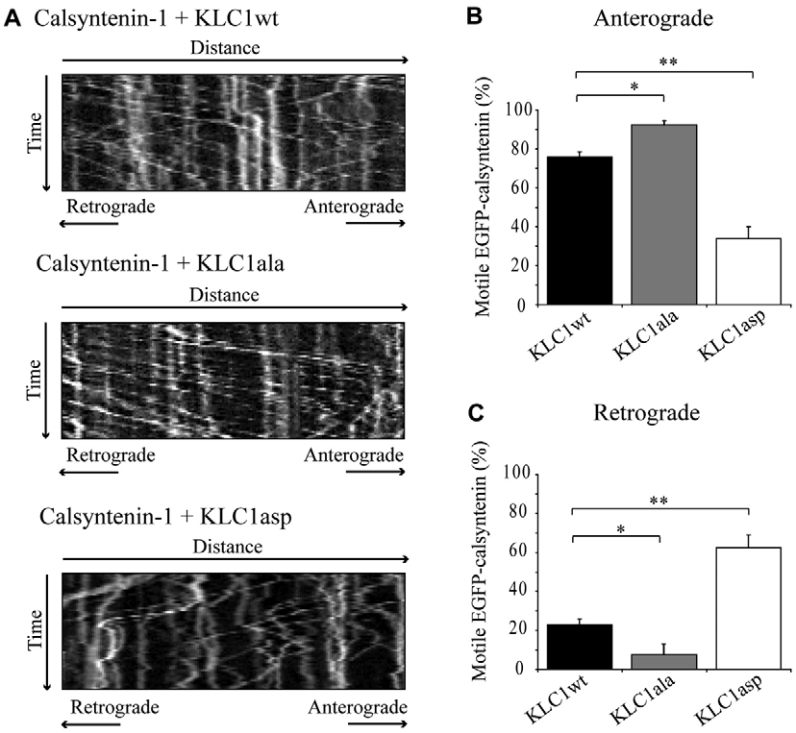

Fig. 7. Mutation of KLC1ser460 alters axonal transport of calsyntenin-1. Rat cortical neurons were co-transfected with EGFP–calsyntenin-1 and FLAG–KLC1wt (KLC1wt), FLAG–KLC1ser460ala (KLC1ala) or FLAG–KLC1ser460asp (KLC1asp), and calsyntenin-1 transport was recorded in time-lapse through visualisation of the EGFP tag. (**A**) Representative kymographs for each transfection are shown. (**B**,**C**) Histograms showing the number (expressed as a normalised percentage) of EGFP–calsyntenin-1 particles moving in both anterograde and retrograde directions in the presence of KLC1wt, KLC1ala or KLC1asp. KLC1ala increases, whereas KLC1asp decreases, anterograde movement, compared with that in KLC1wt; corresponding changes in retrograde movements are observed. Data were analysed by one-way ANOVA with LSD post-hoc test (*P<0.05; **P<0.001) for n=9 cells for each transfection from three independent experiments. Error bars are s.e.m.

whereas mutation to an aspartate residue, to mimic permanent phosphorylation, reduced this binding. We also present evidence that KLC1ser460 is phosphorylated by ERK, and show that inhibition of ERK promotes binding of KLC1 and kinesin-1 motors to calsyntenin-1. Finally, we show that mutation of KLC1ser460 influences its colocalisation with calsyntenin-1 and the transport of calsyntenin-1.

Interestingly, mutation of KLC1ser460 to an aspartate residue reduced but did not eliminate the binding of calsyntenin-1. Likewise, we still observed significant (albeit reduced) colocalisation of KLC1ser460asp with calsyntenin-1 in transfected CV-1 cells; anterograde transport of calsyntenin-1 in KLC1ser460asp co-transfected neurons was also reduced but not eliminated. These observations suggest that, although the phosphorylation state of KLC1ser460 modulates binding and transport of calsyntenin-1, phosphorylation of this residue is not sufficient to completely detach calsyntenin-1 from kinesin-1 so as to abrogate transport. Such reduction, but not elimination, of calsyntenin-1 binding to KLC1ser460asp probably explains the presence of EGFP–calsyntenin-1 in axons of KLC1ser460asp co-transfected neurons; complete elimination of binding might be predicted to block entry of calsyntenin-1 into axons. Support for this notion comes from analyses of the axonal transport of YFP-tagged amyloid precursor protein (APP) in *KLC1*-heterozygous-knockout neurons (i.e. upon a 50% reduction in *KLC1* expression). This reduction in *KLC1* expression likewise decreases but does not eliminate anterograde transport of APP as transfected APP–YFP is still present in axons (Stokin et al., 2005).

The above evidence suggests that there are other mechanisms that influence the release of calsyntenin-1 from KLC1. These might involve the phosphorylation of additional, as yet unidentified sites, in KLC1 or even alterations to the calsyntenin-1 cargo itself. Indeed, alterations to cargoes, including changes in their phosphorylation, have been shown to influence their transport and binding to molecular motors including kinesins (Ackerley et al., 2003; Jung et al., 2005; Wagner et al., 2004; Yates et al., 2009). A fuller understanding of calsyntenin-1 transport will require more detailed knowledge of such post-translational modifications to KHC, KLC1 and calsyntenin-1.

Mutation of KLC1ser460 did not influence the binding of KLC1 to HAP1A, CRMP2, JIP1 or Kidins220 (ARMS). Moreover, the intracellular distribution of HAP1A was unaffected by co-transfection with KLC1ser460ala or KLC1ser460asp. Although the TPR domains of KLC1 are involved in binding cargoes, the precise details of KLC1–cargo interactions are not properly understood and there is evidence that cargo-specific differences exist. A region of KLC1 spanning all six TPR domains but excluding the heptad repeats has been shown to bind calsyntenin-1 and CRMP2 (Araki et al., 2007; Kimura et al., 2005; Konecna et al., 2006). Mutational analyses of KLC1 have indicated that its binding to JIP1 requires sequences that are C-terminal to leucine347 (i.e. the fourth TPR domain) (Hammond et al., 2008). Likewise, the C-terminal region of KLCs, containing the TPR domains, binds to HAP1A (McGuire et al., 2005). However, the KLC1 interaction with Kidins220 involves a C-terminal portion of the heptad repeat region and only the first two TPR domains (Bracale et al., 2007). KLC1ser460 resides within a linker region between the fifth and the sixth TPR domains (Fig. 1A), and, as such, its phosphorylation might be predicted to not influence binding to Kidins220 given that this involves other regions of KLC1. However, how phosphorylation of this linker region influences the overall structure of KLC1, and the TPR domain region in particular, is not clear at this stage. Regardless, our finding that mutation of KLC1ser460 modulates binding to calsyntenin-1, but not four other cargoes, supports the notion that phosphorylation of this residue exerts at least some measure of selectivity on cargo transport.

Neurons display the highest levels of expression of both calsyntenin-1 and KLC1 (Hintsch et al., 2002; Rahman et al.,

1998), and KLC1 has been shown to mediate transport of calsyntenin-1 in neurons (Araki et al., 2007; Konecna et al., 2006). However, there is also evidence that KLC2 can bind to calsyntenin-1 (Araki et al., 2007; Konecna et al., 2006). Interestingly, serine 460 and its surrounding sequences are highly conserved in KLC2 (KLC2ser445), and sequencing of the phosphoproteome has shown that KLC2ser445 can also undergo phosphorylation (Beausoleil et al., 2006; Cantin et al., 2008; Dephoure et al., 2008). Thus, it is possible that KLC2 also mediates attachment of calsyntenin-1 to kinesin-1, particularly in non-neuronal cells where KLC1 is absent or expressed at low levels, and that phosphorylation of KLC2ser445 modulates calsyntenin-1 transport in a fashion similar to KLC1ser460.

In addition to binding KLC1, calsyntenin-1 also interacts with X11β (also known as ABPA2; amyloid-β precursor-protein-binding A2) (Araki et al., 2003). The interaction between calsyntenin-1 and X11β can facilitate formation of a tripartite complex that also contains APP (Araki et al., 2003). APP is processed to release amyloid-β (Aβ) peptide, which is deposited in the brains of Alzheimer's disease patients and is believed to be a key pathogenic event in Alzheimer's disease (for a review, see Walsh and Selkoe, 2004). X11β binds directly to APP and elevation of X11β inhibits Aβ production (Araki et al., 2003; Lee et al., 2004; Mitchell et al., 2009), although the mechanisms underlying this effect are not fully understood. However, defective axonal transport has been linked to increased Aβ production (De Vos et al., 2008; Stokin et al., 2005), and there is evidence that calsyntenin-1 mediates the attachment of kinesin-1 to APP-containing vesicles (Ludwig et al., 2009). Calsyntenin-1 can also influence APP processing and Aβ production, possibly through X11β (Araki et al., 2003; Ludwig et al., 2009). As such, the phosphorylation of KLC1ser460, which we describe here as a regulator of binding between KLC1 and calsyntenin-1, might also have an impact upon APP transport and its processing to produce Aβ in Alzheimer's disease.

Materials and Methods

Plasmids, mutagenesis and siRNAs

N-terminally FLAG-tagged mouse KLC1 was generated by PCR using primers 5′-GCGGCGGAATTCATGGACTACAAAGACGATGACGACAAGGTGTACATAAAGGAAGAGAAGCTGGAG-3′ and 5′-CGCCGCGAATTCCTAGGCTTCCTCCCCTCCGTCAGGGCCACTC-3′, and was cloned into the mammalian expression vector pCI-neo (Promega) as an *Eco*R1 fragment. KCL1ser460 was mutated into alanine and aspartate using a QuikChange XL site-directed mutagenesis kit (Stratagene) according to the manufacturer's instructions. Mutagenic oligonucleotides were: KLC1ser460ala, 5′-GCCTGCAAAGTGGACGCTCCCACCGTCACAACC-3′ and 5′-GGTTGTGACGGTGGGAGCGTCCACTTTGCAGGC-3′; and KLC1ser460asp, 5′-GCCTGCAAAGTGGACGACCCCACCGTCACAACC-3′ and 5′-GGTTGTGACGGTGGGGTCGTCCACTTTGCAGGC-3′. Mouse JIP1 (Whitmarsh et al., 1998) was N-terminally Myc-tagged by PCR using primers 5′-GCGGCGGAATTCATGGAACAAAAGCTCATTTCTGAAGAGGACTTGGCGGAGCGAGAGAGCGGCCTGGGCGGGGGC-3′ and 5′-CGCCGC GAATTCCTACTCCAAGTAGATATCTTCTGTAGGACA-3′, and cloned into pCI-neo as an *Eco*R1 fragment. DNA sequences were verified by sequencing. EGFP–calsyntenin-1 (Konecna et al., 2006), Myc–HAP1A and EGFP–Myc–HAP1A (Prigge and Schmidt, 2007), EGFP–Kidins220/ARMS (Bracale et al., 2007), GST–KLC1(154–534) (Kamal et al., 2000) and Myc-tagged CRMP2 (Duplan et al., 2010) were as described previously. Verified non-targeting control siRNA and human-specific KLC1 siRNA (5′-AAAGAGCCCUCGAGAUCUA-3′) were purchased from Dharmacon.

Antibodies

Mouse anti-FLAG M2 antibody was from Sigma; rabbit anti-GFP and anti-TGN-46 antibodies were from Abcam; rabbit anti-(active MAPK) antibody was from Promega; rabbit and mouse (clone L2) anti-KLC1 antibodies were from BAbCO and Millipore; mouse anti-KHC H2 and SUK4 antibodies were from Millipore and the DSHB (University of Iowa, Iowa City, IA), respectively; mouse anti-Myc tag (9B11), rabbit polyclonal anti-MSK1-*P* (Thr581), rabbit anti-ATF2-*P* (Thr71) (11G2) and rabbit anti-SAPK/JNK antibodies were obtained from Cell Signaling Technology; rabbit anti-p38 (C-20) and anti-Erk (C-14) antibodies were from Santa Cruz Biotechnology; mouse anti-PDI antibody was from Thermo Scientific; and mouse anti-GM130 antibody was from BD Transduction laboratories. Rabbit anti-KHC (pcp42) antibody was as described previously (Niclas et al., 1994). Anti-calsyntenin-1 antibody was generated by immunising rabbits with GST–calsyntenin-1 (amino acids 878–979) (Konecna et al., 2006) and the antibody was affinity purified prior to use.

Mass spectrometric sequencing

Identification of phosphorylation sites was performed essentially as described previously (Standen et al., 2003). Briefly, FLAG–KLC1 was immunoprecipitated from transfected CHO cells using the FLAG tag, and endogenous KLC1 was immunoprecipitated from rat cortical neurons using the anti-KLC1 antibody (Millipore). The immunoprecipitated proteins were resolved by SDS-PAGE, and the band corresponding to KLC1 was excised and prepared for on-line liquid chromatography tandem mass spectrometry (LC–MS/MS) following trypsin digestion. Chromatographic separations of FLAG–KLC1 were performed using an Ultimate LC system (Dionex, Camberley, UK) coupled to a Q-Tof micro (Waters Corporation); chromatographic separations of endogenous KLC1 were performed using a U3000 system (Dionex) coupled to a 4000 Q-TRAP (Applied Biosystems). Peptides were ionised by electrospray ionisation operating under MassLynx v.4.0 (Q-Tof micro) and Analyst v1.5 (4000 Q-TRAP). The instrument was set to run in automated switching mode, selecting precursor ions on the basis of their intensity and charge state, for sequencing by collision-induced fragmentation. The MS/MS analyses were conducted using collision energy profiles that were chosen on the basis of the mass/charge (*m*/*z*) and the charge state of the peptide, and were optimised for phosphorylated peptides. The mass spectral data was processed into peak lists containing the *m*/*z* value of each precursor ion and the corresponding fragment-ion *m*/*z* values and intensities. Data were searched against a custom-built database using the Mascot searching algorithm (Matrix Science, London, UK). Peptides and phosphorylated peptides of KLC1 were identified by matching the MS/MS data against mass values generated from the theoretical fragmentation of peptides on the basis of the set search criteria. The exact location of phosphorylation within each peptide was determined by the pattern of fragment ions produced.

Cell culture and transfection

CHO cells were grown in Ham's F-12 medium containing 10% fetal bovine serum supplemented with 2 mM glutamine, 100 units/ml penicillin and 100 μg/ml streptomycin (Invitrogen). CV-1 and HEK-293 cells were grown in Dulbecco's modified Eagle's medium (DMEM) containing 10% fetal bovine serum supplemented with 2 mM glutamine, 100 units/ml penicillin and 100 μg/ml streptomycin. CHO cells were transfected using Lipofectamine (Invitrogen), CV-1 cells using Exgen500 (Fermentas) and HEK-293 cells with Lipofectamine 2000 (Invitrogen), according to the manufacturers' instructions. For kinase inhibition experiments, cells were treated with either vehicle or 20 μM U0126 (Calbiochem), 10 μM SB203580 (Tocris Biosciences) or 30 μM SP600125 (Tocris Biosciences) for 2 hours before analysis. Cortical neurons were obtained from embryonic day 18 rat embryos and cultured and transfected with Lipofectamine 2000 (Invitrogen) as described previously (Ackerley et al., 2000; Yates et al., 2009).

SDS-PAGE and immunoblotting

Cells were harvested for SDS-PAGE by washing with PBS pre-warmed to 37°C, scraping into SDS-PAGE sample buffer and immediately heating to 100°C. Samples were separated on either 8% or 10 % (w/v) acrylamide gels, transferred onto Protran nitrocellulose membranes (Schleicher & Schuell) using a Transblot system (BioRad) and, following blocking, the blots were then probed with primary antibodies. Following washing, the blots were further probed with horseradish peroxidase-conjugated goat secondary antibodies against mouse or rabbit Ig, and developed using an enhanced chemiluminescence system (GE Healthcare). Signals on immunoblots were quantified using ImageJ (National Institutes of Health), after scanning with an Epson Precision V700 Photo scanner, essentially as described by us in previous studies (Lee et al., 2003). To ensure the signals obtained were within the linear range, the mean background-corrected optical density (OD) of each signal was interpolated for an OD calibration curve created using a calibrated OD step tablet (Kodak). Only film exposures that gave OD signals within the linear range of the OD calibration curve were used for statistical analyses. For quantification of the signals of calsyntenin-1 bound to KLC1 in the immunoprecipitation assays, the signals for the co-immunoprecipitating calsyntenin-1 were normalised to the KLC1 immunoprecipitation signals, and the signals for the co-immunoprecipitating KLC1 were normalised to the calsyntenin-1 immunoprecipitation signals. Data were analysed by using one-way ANOVA tests with Fisher's LSD (least significant difference) post-hoc test, or by using a Student's *t*-test, as indicated.

Immunoprecipitation

For immunoprecipitation assays, transfected cells were lysed in ice-cold immunoprecipitation buffer comprising 20 mM Tris-HCl, pH 7.5, 150 mM NaCl, 0.5% Triton X-100, 0.5 mM sodium orthovanadate, 1 mM phenylmethanesulphonyl fluoride (PMSF), 20 mM sodium fluoride and protease inhibitors (Complete, Roche) for 30 minutes. After centrifugation at 16,000 ***g*** for 30 min at 4°C, the supernatants were pre-cleared with protein G–Sepharose beads (Sigma) for 1 hour at 4°C (and then incubated with primary antibodies for 16 hours at 4°C). Antibodies were

captured with protein G–Sepharose beads and, following washing with immunoprecipitation buffer, bound proteins were eluted by incubation in SDS-PAGE sample buffer and heating at 100°C. Samples were then analysed by immunoblotting.

In vitro phosphorylation studies

GST–KLC1(154–534) and GST–KLC1(154–534)ser460ala substrates were expressed in *E. coli* BL21 cells and purified using glutathione–Sepharose 4B beads (GE Healthcare); recombinant proteins were released from the GST moiety by incubation with thrombin according to the manufacturer's instructions (GE Healthcare). Substrates were phosphorylated using recombinant activated GST–ERK (Cell Signaling Technology). Briefly, 2 µg of each substrate was incubated with 24 ng of GST–ERK and 0.185 MBq [γ^{32}P]ATP in 25 mM Tris-HCl, pH 7.5, containing 10 mM $MgCl_2$, 5 mM 2-glycerophosphate, 0.1 mM sodium orthovanadate, 2 mM dithiothreitol and 20 µM ATP for 20 minutes at 30°C in a final volume of 30 µl. The reactions were stopped by adding SDS-PAGE sample buffer and heating to 100°C. Samples were separated on a 10% (w/v) acrylamide gel, and the gels were stained with Brilliant Blue G colloidal concentrate (Sigma) and subjected to autoradiography.

Immunofluorescence and time-lapse microscopy

Cells were analysed by immunostaining at 24 hours post-transfection. Cells were fixed in 4% formaldehyde in PBS for 20 minutes, quenched with 0.05 M NH_4Cl for 15 minutes, washed in PBS and then permeabilised with 0.2% Triton X-100 in PBS for 5 minutes. Following blocking with 5% goat serum (Sigma) in PBS for 30 minutes, the samples were probed with primary antibodies diluted in blocking solution (PBS containing 5% goat serum). KLC1 was detected using the FLAG tag and EGFP–calsyntenin-1 and EGFP–HAP1A through the EGFP moieties. Primary antibodies were then detected using goat antibodies against mouse or rabbit Igs coupled to Alexa Fluor 546 or 633 (Invitrogen). For intensity correlation analysis, images were captured using a Zeiss LSM510Meta confocal microscope equipped with a 63×, Plan-Apochromat 1.4 NA objective (Zeiss), and analysed using ImageJ with the intensity correlation analysis plug-in. Further calculations and statistical analysis were performed using Excel (Microsoft Corporation) and SPSS 15 (IBM). Light-microscopy was performed using a Leica DM5000B microscope with 63× HCX PL Fluotar phase objective.

Live microscopy of EGFP–calsyntenin-1 vesicular transport was performed with an Axiovert S100 microscope (Zeiss) equipped with a Lambda LS Xenon-Arc light source (Sutter Instrument Company, Novato, CA), a GFP filterset (Chroma Technology, Rockingham, VT), a 100× Plan-Apochromat 1.4 NA objective (Zeiss), a Lambda 10-3 filter wheel (Sutter Instrument Company) and a Photometrics Cascade-II 512B High Speed EMCCD camera (Photometrics, Tucson, AZ). At 16–24 hours post-transfection, the cells were transferred into a Ludin imaging chamber (Life Imaging Systems, Basel, Switzerland) that was mounted onto the stage of the microscope. The cells were maintained at 37°C using an objective heater (IntraCell, Royston, UK) and 'The Box' microscope temperature control system (Life Imaging Systems). Vesicle movements were recorded for 5 minutes, with a 1-second time-lapse interval, using MetaMorph software (Molecular Devices). A movement was defined as a displacement of a particle of at least 2 µm, without reversal of direction of more than 2 µm or pausing for longer than 5 seconds. Image analysis was performed with ImageJ and velocities were determined using the SlopeToVelocity plug-in (De Vos and Sheetz, 2007).

This work was supported by grants from the UK Medical Research Council, Wellcome Trust, Alzheimer's Research Trust and European Union 7th Framework Programme for RTD, Project MitoTarget (Grant Agreement HEALTH-F2-2008-223388). We thank Peter Sonderegger (University of Zurich, Zurich, Switzerland) for calsyntenin-1 clones, Ed Schmidt (Montana State University, Bozeman, MT) for HAP1A clones, Giampietro Schiavo (Cancer Research UK, London, UK) for the EGFP–Kidins220 clone, Roger Davis (University of Massachusetts, Worcester, MA) for the JIP1 clone, Brigitte Pettmann (Inmed, Marseille, France) for the CRMP2 clone, Lawrence Goldstein (University of California, San Diego,CA) for the GST–KLC1 clone and Ron Vale (University of California, San Francisco, CA) for the anti-KHC antibody. We also thank Helen Byers, Malcolm Ward, Steven Lynham and Mireia Fernandez-Ocana (Proteome Sciences, Kings College, London, UK) for assistance with mass spectrometry. Deposited in PMC for release after 6 months.

Supplementary material available online at
http://jcs.biologists.org/cgi/content/full/124/7/1032/DC1

References

Ackerley, S., Grierson, A. J., Brownlees, J., Thornhill, P., Anderton, B. H., Leigh, P. N., Shaw, C. E. and Miller, C. C. J. (2000). Glutamate slows axonal transport of neurofilaments in transfected neurons. *J. Cell Biol.* **150**, 165-175.

Ackerley, S., Thornhill, P., Grierson, A. J., Brownlees, J., Anderton, B. H., Leigh, P. N., Shaw, C. E. and Miller, C. C. J. (2003). Neurofilament heavy chain side-arm phosphorylation regulates axonal transport of neurofilaments. *J. Cell Biol.* **161**, 489-495.

Araki, Y., Tomita, S., Yamaguchi, H., Miyagi, N., Sumioka, A., Kirino, Y. and Suzuki, T. (2003). Novel cadherin-related membrane proteins, Alcadeins, enhance the X11-like protein-mediated stabilization of amyloid beta-protein precursor metabolism. *J. Biol. Chem.* **278**, 49448-49458.

Araki, Y., Kawano, T., Taru, H., Saito, Y., Wada, S., Miyamoto, K., Kobayashi, H., Ishikawa, H. O., Ohsugi, Y., Yamamoto, T. et al. (2007). The novel cargo Alcadein induces vesicle association of kinesin-1 motor components and activates axonal transport. *EMBO J.* **26**, 1475-1486.

Beausoleil, S. A., Villen, J., Gerber, S. A., Rush, J. and Gygi, S. P. (2006). A probability-based approach for high-throughput protein phosphorylation analysis and site localization. *Nat. Biotechnol.* **24**, 1285-1292.

Bowman, A. B., Kamal, A., Ritchings, B. W., Philp, A. V., McGrail, M., Gindhart, J. G. and Goldstein, L. S. (2000). Kinesin-dependent axonal transport is mediated by the sunday driver (SYD) protein. *Cell* **103**, 583-594.

Bracale, A., Cesca, F., Neubrand, V. E., Newsome, T. P., Way, M. and Schiavo, G. (2007). Kidins220/ARMS is transported by a kinesin-1-based mechanism likely to be involved in neuronal differentiation. *Mol. Biol. Cell* **18**, 142-152.

Cantin, G. T., Yi, W., Lu, B., Park, S. K., Xu, T., Lee, J. D. and Yates, J. R., 3rd (2008). Combining protein-based IMAC, peptide-based IMAC, and MudPIT for efficient phosphoproteomic analysis. *J. Proteome Res.* **7**, 1346-1351.

Daub, H., Olsen, J. V., Bairlein, M., Gnad, F., Oppermann, F. S., Korner, R., Greff, Z., Keri, G., Stemmann, O. and Mann, M. (2008). Kinase-selective enrichment enables quantitative phosphoproteomics of the kinome across the cell cycle. *Mol. Cell* **31**, 438-448.

De Vos, K. J. and Sheetz, M. P. (2007). Visualization and quantification of mitochondrial dynamics in living animal cells. *Methods Cell Biol.* **80**, 627-682.

De Vos, K., Severin, F., Van Herreweghe, F., Vancompernolle, K., Goossens, V., Hyman, A. and Grooten, J. (2000). Tumor necrosis factor induces hyperphosphorylation of kinesin light chain and inhibits kinesin-mediated transport of mitochondria. *J. Cell Biol.* **149**, 1207-1214.

De Vos, K. J., Chapman, A. L., Tennant, M. E., Manser, C., Tudor, E. L., Lau, K. F., Brownlees, J., Ackerley, S., Shaw, P. J., McLoughlin, D. M. et al. (2007). Familial amyotrophic lateral sclerosis-linked SOD1 mutants perturb fast axonal transport to reduce axonal mitochondria content. *Hum. Mol. Genet.* **16**, 2720-2728.

De Vos, K. J., Grierson, A. J., Ackerley, S. and Miller, C. C. J. (2008). Role of axonal transport in neurodegenerative diseases. *Annu. Rev. Neurosci.* **31**, 151-173.

DeBoer, S. R., You, Y., Szodorai, A., Kaminska, A., Pigino, G., Nwabuisi, E., Wang, B., Estrada-Hernandez, T., Kins, S., Brady, S. T. et al. (2008). Conventional kinesin holoenzymes are composed of heavy and light chain homodimers. *Biochemistry* **47**, 4535-4543.

Dephoure, N., Zhou, C., Villen, J., Beausoleil, S. A., Bakalarski, C. E., Elledge, S. J. and Gygi, S. P. (2008). A quantitative atlas of mitotic phosphorylation. *Proc. Natl. Acad. Sci. USA* **105**, 10762-10767.

Dompierre, J. P., Godin, J. D., Charrin, B. C., Cordelieres, F. P., King, S. J., Humbert, S. and Saudou, F. (2007). Histone deacetylase 6 inhibition compensates for the transport deficit in Huntington's disease by increasing tubulin acetylation. *J. Neurosci.* **27**, 3571-3583.

Duplan, L., Bernard, N., Casseron, W., Dudley, K., Thouvenot, E., Honnorat, J., Rogemond, V., De Bovis, B., Aebischer, P., Marin, P. et al. (2010). Collapsin response mediator protein 4a (CRMP4a) is upregulated in motoneurons of mutant SOD1 mice and can trigger motoneuron axonal degeneration and cell death. *J. Neurosci.* **30**, 785-796.

Gauger, A. K. and Goldstein, L. S. (1993). The Drosophila kinesin light chain. Primary structure and interaction with kinesin heavy chain. *J. Biol. Chem.* **268**, 13657-13666.

Guillaud, L., Wong, R. and Hirokawa, N. (2007). Disruption of KIF17-Mint1 interaction by CaMKII-dependent phosphorylation: a molecular model of kinesin-cargo release. *Nat. Cell Biol.* **10**, 19-29.

Hammond, J. W., Griffin, K., Jih, G. T., Stuckey, J. and Verhey, K. J. (2008). Co-operative versus independent transport of different cargoes by Kinesin-1. *Traffic* **9**, 725-741.

Hintsch, G., Zurlinden, A., Meskenaite, V., Steuble, M., Fink-Widmer, K., Kinter, J. and Sonderegger, P. (2002). The calsyntenins – a family of postsynaptic membrane proteins with distinct neuronal expression patterns. *Mol. Cell Neurosci.* **21**, 393-409.

Hirokawa, N. and Noda, Y. (2008). Intracellular transport and kinesin superfamily proteins, KIFs: structure, function, and dynamics. *Physiol. Rev.* **88**, 1089-1118.

Hollenbeck, P. J. (1993). Phosphorylation of neuronal kinesin heavy and light chains in vivo. *J. Neurochem.* **60**, 2265-2275.

Ichimura, T., Wakamiya-Tsuruta, A., Itagaki, C., Taoka, M., Hayano, T., Natsume, T. and Isobe, T. (2002). Phosphorylation-dependent interaction of kinesin light chain 2 and the 14-3-3 protein. *Biochemistry* **41**, 5566-5572.

Jung, C., Lee, S., Ortiz, D., Zhu, Q., Julien, J. P. and Shea, T. B. (2005). The high and middle molecular weight neurofilament subunits regulate the association of neurofilaments with kinesin: Inhibition by phosphorylation of the high molecular weight subunit. *Brain Res. Mol. Brain Res.* **141**, 151-155.

Kamal, A., Stokin, G. B., Yang, Z. H., Xia, C. H. and Goldstein, L. S. B. (2000). Axonal transport of amyloid precursor protein is mediated by direct binding to the kinesin light chain subunit of kinesin-I. *Neuron* **28**, 449-459.

Kimura, T., Watanabe, H., Iwamatsu, A. and Kaibuchi, K. (2005). Tubulin and CRMP-2 complex is transported via Kinesin-1. *J. Neurochem.* **93**, 1371-1382.

Konecna, A., Frischknecht, R., Kinter, J., Ludwig, A., Steuble, M., Meskenaite, V., Indermuhle, M., Engel, M., Cen, C., Mateos, J. M. et al. (2006). Calsyntenin-1 docks vesicular cargo to kinesin-1. *Mol. Biol. Cell* **17**, 3651-3663.

Lee, J. H., Lau, K. F., Perkinton, M. S., Standen, C. L., Shemilt, S. J., Mercken, L., Cooper, J. D., McLoughlin, D. M. and Miller, C. C. (2003). The neuronal adaptor protein X11alpha reduces Abeta levels in the brains of Alzheimer's APPswe Tg2576 transgenic mice. *J. Biol. Chem.* **278**, 47025-47029.

Lee, J. H., Lau, K. F., Perkinton, M. S., Standen, C. L., Rogelj, B., Falinska, A., McLoughlin, D. M. and Miller, C. C. (2004). The neuronal adaptor protein X11beta reduces Abeta levels and amyloid plaque formation in the brains of transgenic mice. *J. Biol. Chem.* **279**, 49099-49104.

Lee, K. D. and Hollenbeck, P. J. (1995). Phosphorylation of kinesin in vivo correlates with organelle association and neurite outgrowth. *J. Biol. Chem.* **270**, 5600-5605.

Li, Q., Lau, A., Morris, T. J., Guo, L., Fordyce, C. B. and Stanley, E. F. (2004). A syntaxin 1, Galpha(o), and N-type calcium channel complex at a presynaptic nerve terminal: analysis by quantitative immunocolocalization. *J. Neurosci.* **24**, 4070-4081.

Lindesmith, L., McIlvain, J. M., Jr, Argon, Y. and Sheetz, M. P. (1997). Phosphotransferases associated with the regulation of kinesin motor activity. *J. Biol. Chem.* **272**, 22929-22933.

Ludwig, A., Blume, J., Diep, T. M., Yuan, J., Mateos, J. M., Leuthauser, K., Steuble, M., Streit, P. and Sonderegger, P. (2009). Calsyntenins mediate TGN exit of APP in a Kinesin-1-dependent manner. *Traffic* **10**, 572-589.

Matthies, H. J., Miller, R. J. and Palfrey, H. C. (1993). Calmodulin binding to and cAMP-dependent phosphorylation of kinesin light chains modulate kinesin ATPase activity. *J. Biol. Chem.* **268**, 11176-11187.

McGuire, J. R., Rong, J., Li, S. H. and Li, X. J. (2005). Interaction of huntingtin-associated protein-1 with kinesin light chain: Implications in intracellular trafficking in neurons. *J. Biol. Chem.* **281**, 3552-3559.

Mitchell, J. C., Ariff, B. B., Yates, D. M., Lau, K. F., Perkinton, M. S., Rogelj, B., Stephenson, J. D., Miller, C. C. and McLoughlin, D. M. (2009). X11beta rescues memory and long-term potentiation deficits in Alzheimer's disease APPswe Tg2576 mice. *Hum. Mol. Genet.* **18**, 4492-4500.

Morfini, G., Szebenyi, G., Elluru, R., Ratner, N. and Brady, S. T. (2002). Glycogen synthase kinase 3 phosphorylates kinesin light chains and negatively regulates kinesin-based motility. *EMBO J.* **21**, 281-293.

Morfini, G. A., You, Y. M., Pollema, S. L., Kaminska, A., Liu, K., Yoshioka, K., Bjorkblom, B., Coffey, E. T., Bagnato, C., Han, D. et al. (2009). Pathogenic huntingtin inhibits fast axonal transport by activating JNK3 and phosphorylating kinesin. *Nat. Neurosci.* **12**, 864-871.

Niclas, J., Navone, F., Hom-Booher, N. and Vale, R. D. (1994). Cloning and localization of a conventional kinesin motor expressed exclusively in neurons. *Neuron* **12**, 1059-1072.

Prigge, J. R. and Schmidt, E. E. (2007). HAP1 can sequester a subset of TBP in cytoplasmic inclusions via specific interaction with the conserved TBP(CORE). *BMC Mol. Biol.* **8**, 76.

Rahman, A., Friedman, D. S. and Goldstein, L. S. (1998). Two kinesin light chain genes in mice. Identification and characterization of the encoded proteins. *J. Biol. Chem.* **273**, 15395-15403.

Reed, N. A., Cai, D., Blasius, T. L., Jih, G. T., Meyhofer, E., Gaertig, J. and Verhey, K. J. (2006). Microtubule acetylation promotes kinesin-1 binding and transport. *Curr. Biol.* **16**, 2166-2172.

Sato-Yoshitake, R., Yorifuji, H., Inagaki, M. and Hirokawa, N. (1992). The phosphorylation of kinesin regulates its binding to synaptic vesicles. *J. Biol. Chem.* **267**, 23930-23936.

Stagi, M., Gorlovoy, P., Larionov, S., Takahashi, K. and Neumann, H. (2006). Unloading kinesin transported cargoes from the tubulin track via the inflammatory c-Jun N-terminal kinase pathway. *FASEB J.* **20**, 2573-2575.

Standen, C. L., Perkinton, M. S., Byers, H. L., Kesavapany, S., Lau, K. F., Ward, M., McLoughlin, D. and Miller, C. C. (2003). The neuronal adaptor protein Fe65 is phosphorylated by mitogen-activated protein kinase (ERK1/2). *Mol. Cell Neurosci.* **24**, 851-857.

Stock, M. F., Guerrero, J., Cobb, B., Eggers, C. T., Huang, T. G., Li, X. and Hackney, D. D. (1999). Formation of the compact confomer of kinesin requires a COOH-terminal heavy chain domain and inhibits microtubule-stimulated ATPase activity. *J. Biol. Chem.* **274**, 14617-14623.

Stokin, G. B., Lillo, C., Falzone, T. L., Brusch, R. G., Rockenstein, E., Mount, S. L., Raman, R., Davies, P., Masliah, E., Williams, D. S. et al. (2005). Axonopathy and transport deficits early in the pathogenesis of Alzheimer's disease. *Science* **307**, 1282-1288.

Tudor, E. L., Galtrey, C. M., Perkinton, M. S., Lau, K. F., De Vos, K. J., Mitchell, J. C., Ackerley, S., Hortobagyi, T., Vamos, E., Leigh, P. N. et al. (2010). Amyotrophic lateral sclerosis mutant VAPB transgenic mice develop TDP-43 pathology. *Neuroscience* **167**, 774-785.

Verhey, K. J., Lizotte, D. L., Abramson, T., Barenboim, L., Schnapp, B. J. and Rapoport, T. A. (1998). Light chain-dependent regulation of Kinesin's interaction with microtubules. *J. Cell Biol.* **143**, 1053-1066.

Verhey, K. J., Meyer, D., Deehan, R., Blenis, J., Schnapp, B. J., Rapoport, T. A. and Margolis, B. (2001). Cargo of kinesin identified as JIP scaffolding proteins and associated signaling molecules. *J. Cell Biol.* **152**, 959-970.

Wagner, O. I., Ascano, J., Tokito, M., Leterrier, J. F., Janmey, P. A. and Holzbaur, E. L. (2004). The interaction of neurofilaments with the microtubule motor cytoplasmic dynein. *Mol. Biol. Cell* **15**, 5092-5100.

Walsh, D. M. and Selkoe, D. J. (2004). Deciphering the molecular basis of memory failure in Alzheimer's disease. *Neuron* **44**, 181-193.

Whitmarsh, A. J., Cavanagh, J., Tournier, C., Yasuda, J. and Davis, R. J. (1998). A mammalian scaffold complex that selectively mediates MAP kinase activation. *Science* **281**, 1671-1674.

Wozniak, M. J. and Allan, V. J. (2006). Cargo selection by specific kinesin light chain 1 isoforms. *EMBO J.* **25**, 5457-5468.

Yates, D. M., Manser, C., De Vos, K. J., Shaw, C. E., McLoughlin, D. M. and Miller, C. C. (2009). Neurofilament subunit (NFL) head domain phosphorylation regulates axonal transport of neurofilaments. *Eur. J. Cell Biol.* **88**, 193-202.

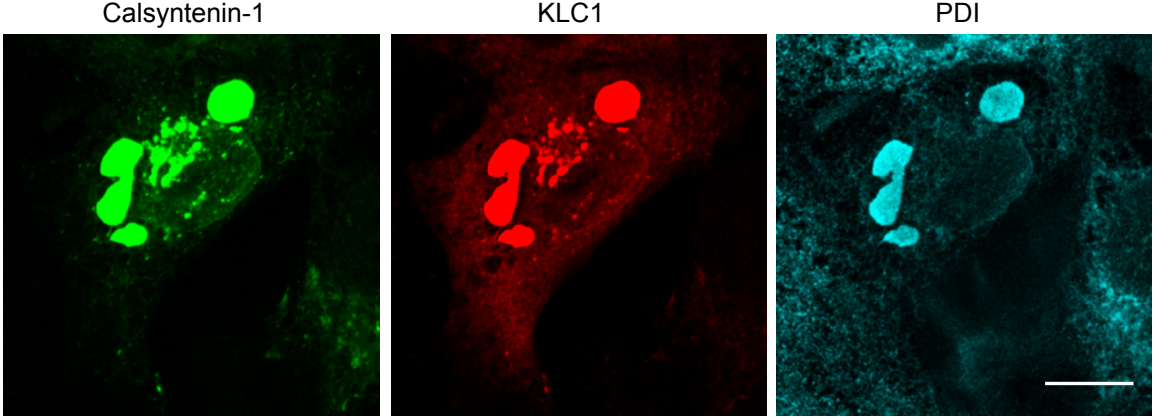
Calsyntenin-1
KLC1
PDI

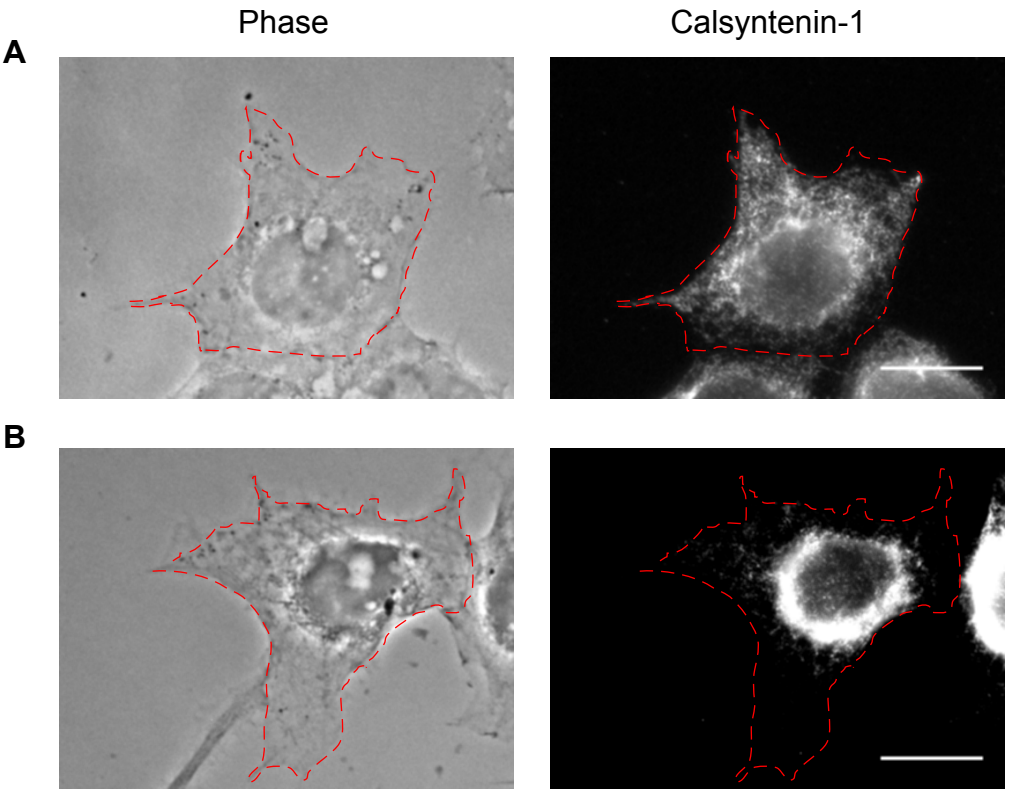
Phase
Calsyntenin-1
A
B

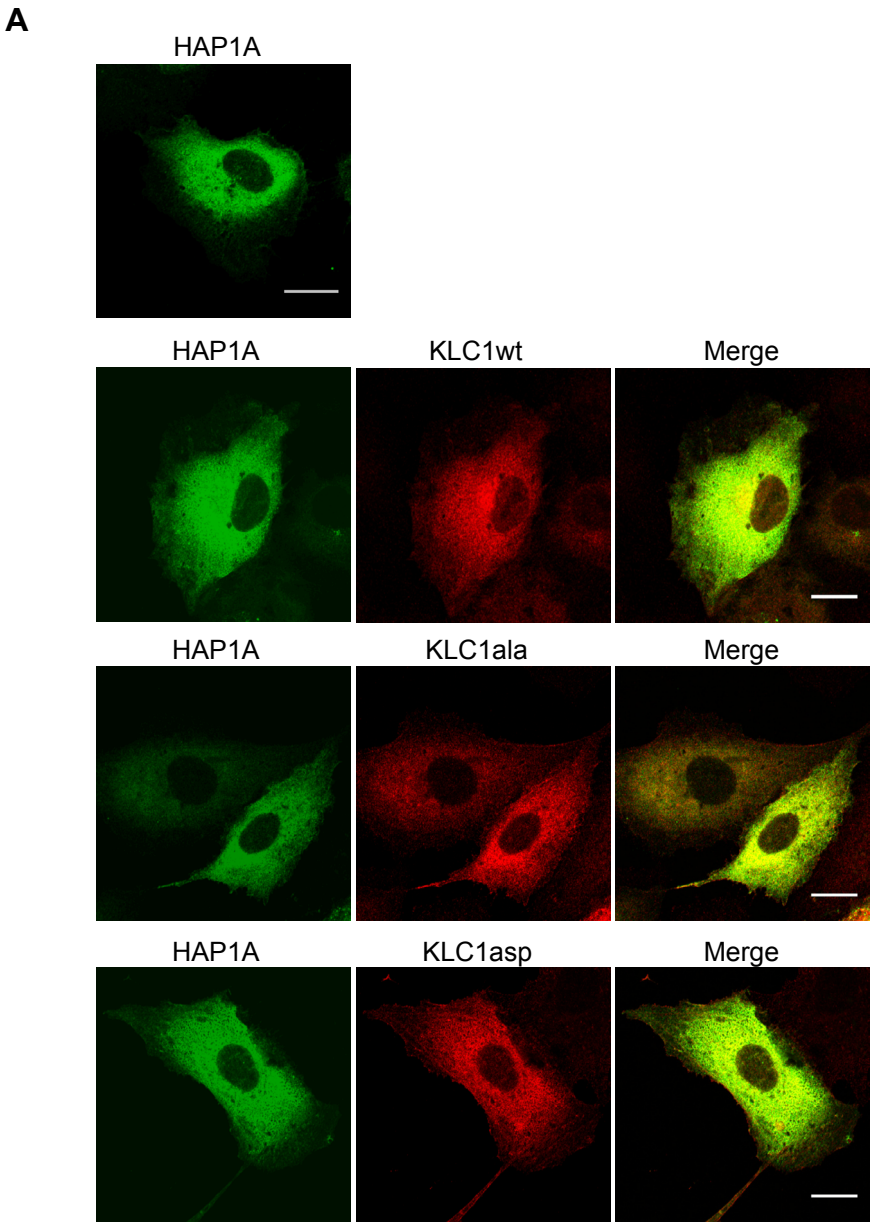
A
HAP1A
HAP1A
KLC1wt
Merge
HAP1A
KLC1ala
Merge
HAP1A
KLC1asp
Merge
B
ICQ (HAP1A-KLC1)
0.5
0.4
0.3
0.2
0.1
0
ns
ns
KLC1wt
KLC1ala
KLC1asp